HYDRODYNAMIC CHARACTERISTICS OF PSEUDO-LIQUEFACTION OF GRANULAR MATERIALS IN CONICAL AND CONICO-CYLINDRICAL EQUIPMENT

N. I. Gel'perin, V. G. Aynshteyn,
E. N. Gel'perin, and S. D. L'vova

(NASA-TT-F-16242) HYDRODYNAMIC CHARACTERISTICS OF PSEUDO-LIQUEFACTION OF GRANULAR MATERIALS IN CONICAL AND CONICO-CYLINDRICAL EQUIPMENT (Kanner (Leo) Associates) 16 p HC $3.25 CSCL 20D G3/34

N75-20651

Unclas
14720

Translation of "Gidrodinamicheskiye osobennosti psevdoozhizheniya zernistykh materialov v konicheskikh i konichesko-tsilindricheskikh apparatakh," Khimiya i tekhnologiya topliv liv i masel, No. 8, 1960, pp. 51-57.

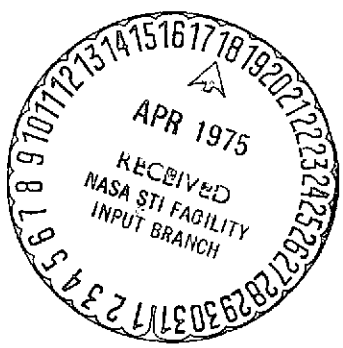

NATIONAL AERONAUTICS AND SPACE ADMINISTRATION
WASHINGTON, D.C. 20546 April 1975

STANDARD TITLE PAGE

1. Report No. NASA TT F-16,242	2. Government Accession No.	3. Recipient's Catalog No.
4. Title and Subtitle HYDRODYNAMIC CHARACTERISTICS OF PSEUDO-LIQUEFACTION OF GRANULAR MATERIALS IN CONICAL AND CONICO-CYLINDRICAL EQUIPMENT		5. Report Date April, 1975 6. Performing Organization Code
7. Author(s) N. I. Gel'perin, V. G. Aynshteyn, E. N. Gel'perin, and S. D. L'vova Moscow Institute of Fine Chemical Technology imeni M. V. Lomonosov		8. Performing Organization Report No. 10. Work Unit No. 11. Contract or Grant No. NASw-2481
9. Performing Organization Name and Address Leo Kanner Associates Redwood City, California 94063		13. Type of Report and Period Covered Translation
12. Sponsoring Agency Name and Address National Aeronautics and Space Administration, Washington, D.C. 20546		14. Sponsoring Agency Code

15. Supplementary Notes

Translation of "Gidrodinamicheskiye osobennosti psevdoozhizh zheniya zernistykh materialov v konicheskikh i konichesko-tsilindricheskikh apparatakh," Khimiya i tekhnologiya topliv i masel, No. 8, 1960, pp. 51-57.

16. Abstract Processes involving fluidized beds of granular material may be based on a conical diffuser as well as gas-distribution grids. In the former case, with proper selection of crosssectional area and cone aperture, the diffusors afford adequate pseudo-liquefaction (fluidization) and may be used separately or with a cylinder. The article reports on experimental study of the hydrodynamic features of granular materials in this kind of equipment, using three quartz sand fractions as the granular material and sand layer heights of 100, 150, 200, and 250 mm.

17. Key Words (Selected by Author(s))	18. Distribution Statement
	Unlimited-Unclassified

19. Security Classif. (of this report)	20. Security Classif. (of this page)	21. No. of Pages	22. Price
Unclassified	Unclassified	16	

NASA-HQ

HYDRODYNAMIC CHARACTERISTICS OF PSEUDO-LIQUEFACTION OF GRANULAR MATERIALS IN CONICAL AND CONICO-CYLINDRICAL EQUIPMENT

/51*

N. I. Gel-perin, V. G. Aynshteyn,
E. N. Gel'perin, and S. D. L'vova

Processes involving pseudo-liquefied (fluidized) layers of granular material are carried out, as is known, mostly in apparatus with gas-distribution grids and vertical walls. The curve of pseudo-liquefaction expressing the dependence of the layer drag (ΔP) on gas velocity in the free section of this kind of apparatus (w) is shown in Fig. 1, 1, where W_p is the velocity at the initial moment of layer expansion, W'_k is the rate of pseudo-liquefaction, and W''_k is the velocity of the gas corresponding to the initial entrainment of the solid phase.

However, the gas-distributing device may be not only a grid, but also a conical diffusor with gas entry through its short section. When the cross-sectional area and the cone aperture are properly selected, the diffusors provide uniform pseudo-liquefaction of the granular layer, and in several cases can be used autonomously or in conjunction with a cylinder as equipment /52 for carrying out technological processes. The hydrodynamics of the fluidized layer in conical and conico-cylindrical equipment thus far has been little investigated, and the present article aims to partially fill this gap.

The hydraulic drag of the fluidized layer in equipment with vertical walls is expressed, as we know, by the equation:

---

* Numbers in the margin indicate pagination in the foreign text.

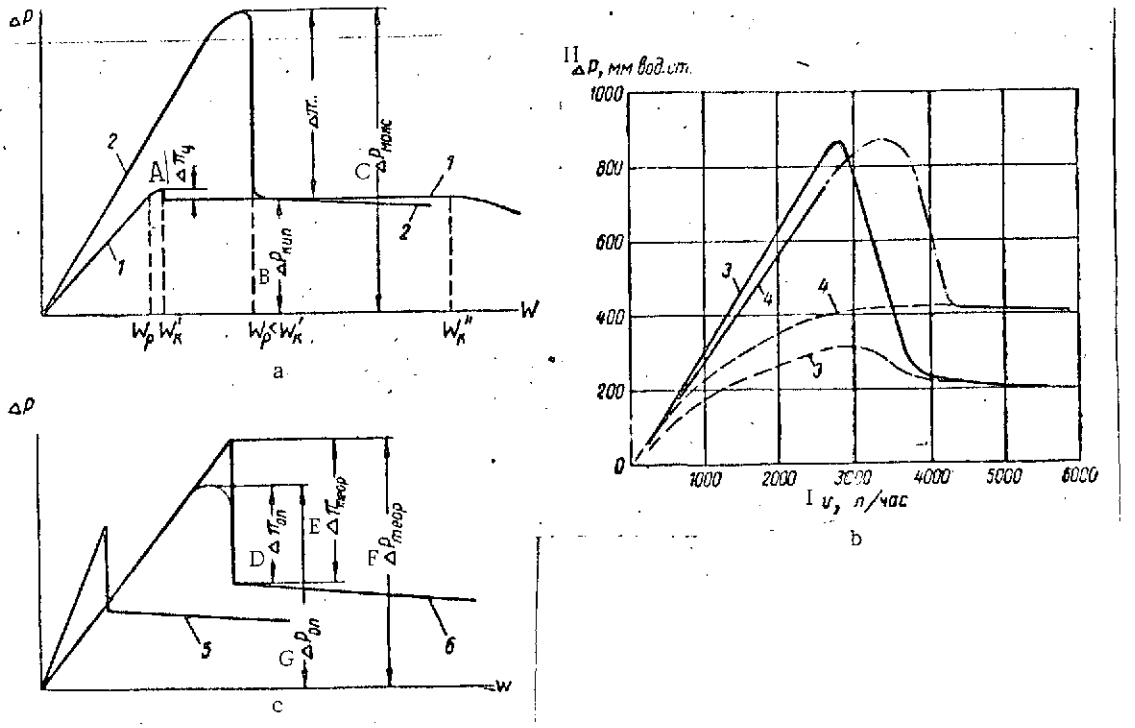

Fig. 1. Curves of pseudo-liquefaction of granular material.
a. In various types of apparatus
b. Based on experimental data
c. Theoretical
1. In equipment with vertical walls
2. In conical equipment
3. As above
4. In conico-cylindrical equipment
5. In equipment with small cone aperture
6. In equipment with large cone aperture and large layer height

KEY:
A. $\Delta\pi_{cyl}$ /cyl = cylindrical/
B. ΔP_{fl} /fl = fluidized/
C. ΔP_{max} /max = maximum/
D. $\Delta\pi_{exp}$ /exp = experimental/
E. $\Delta\pi_{theor}$ /theor = theoretical/
F. ΔP_{theor}
G. ΔP_{exp}
H. ΔP, mm H_2O
I. v, liters/hr

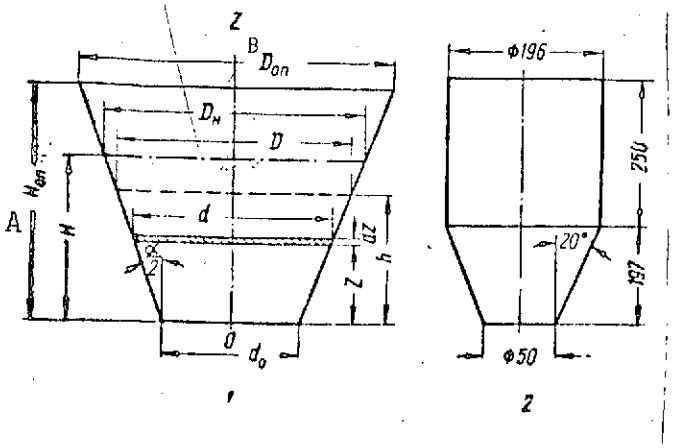

Fig. 2. Shape and dimensions of experimental equipment.
1. Conical
2. Conico-cylindrical
KEY: A. H_{exp}
B. D_{exp}

$$\Delta P_{fl} = \gamma_T(1-\varepsilon)H, \qquad (1)$$ /52

where γ_T is the apparent specific gravity of the solid granular material (the difference between its true specific gravity and the specific gravity of the liquefying gas); ε is the layer porosity; and H is the height of the fluidized layer. In the region in which the still granular layer passes into the state of pseudo-liquefaction /fluidization/, some excess of the pressure drop is observed over the value ΔP_{fl} (Fig. 1 a), which is relatively small in equipment with vertical walls (ΔP_{cyl}), but is very significant in conical equipment ($\Delta\pi_K$ /K = conical/). This effect is accounted for by the fact that in cylindrical (or prismatic) equipment, the entire layer passes into the pseudo-liquefied /fluidized/ state at the moment when a certain distance sufficient for mixing is attained between the layer particles. In conical equipment, the layer passes into the fluidized layer regime only after pseudo-liquefaction of its upper part. Since at this moment the gas velocity in the lower layers considerably exceeds not only W_p, but also W'_k, the pressure drop rises sharply in the layer, and, therefore, $\Delta\pi_k > \Delta\pi_{cyl}$ (Fig. 1, 2).

To study the hydrodynamic features of the fluidized layer in conical equipment, laboratory models were investigated in experiments (Fig. 2).

The height of the cone of these models H_{eq} /eq = equipment/ is 400 mm, the diameter of the lower section d_0 = 50 mm, the diameter of the upper section D_{eq} = 120, 191, 264, 342, and 512 mm, and the cone aperture is 10, 20, 30, 40, and 60°.

In addition, conico-cylindrical equipment whose dimensions are shown in Fig. 2 was investigated.

Three fractions of quartz sand served as the pseudo-liquefied granular material. Their characteristics are given in Table 1.

Experiments with conical equipment were carried out for heights of still sand layers of 100, 150, 200, and 250 mm. In experiments with conico-cylindrical equipment, the cone was filled completely, while the cylindrical part was filled by 50, 100, 150, 200, and 250 mm.

To determine the nature of the dependence of the drag of the fluidized layer in the conical equipment on the gas velocity, let us divide by the distance z from the layer base (Fig. 2) an elementary volume dv that has a cross-sectional area F and height dz. If we assume that the layer porosity ε is constant over its entire area, then the following volume is represented by the fraction of solid particles in the volume dv:

$$dv_т = (1-\varepsilon)\,dv = (1-\varepsilon)\,F\,dz = (1-\varepsilon)\frac{\pi d^2}{4}\,dz.$$

Since /53

$$d = d_0 + 2z\,\mathrm{tg}\,\frac{\alpha}{2},$$

therefore

$$v_т = \frac{G_т}{\gamma_т} = (1-\varepsilon)\int_0^H F\,dz = (1-\varepsilon)\frac{\pi}{4}\int_0^H \left(d_0 + 2z\,\mathrm{tg}\,\frac{\alpha}{2}\right)^2 dz.$$

Hence

$$v_T = \frac{G}{\gamma_T} = \frac{\pi}{4}(1-\varepsilon)H\left(d_0^2 + 2Hd_0 \operatorname{tg}\frac{\alpha}{2} + \frac{4}{3}H^2 \operatorname{tg}^2\frac{\alpha}{2}\right)$$

and

$$\Delta P_{fl} = \gamma_T(1-\varepsilon)H = \frac{G_T}{\frac{\pi}{4}\left(d_0^2 + 2Hd_0 \operatorname{tg}\frac{\alpha}{2} + \frac{4}{3}H^2 \operatorname{tg}^2\frac{\alpha}{2}\right)}, \quad (2)$$

where G_T is the weight of the solid particles in the equipment.

$H \operatorname{tg}\frac{\alpha}{2} = \frac{D_H - d_0}{2}$, therefore Eq. (2) can be represented as

$$\Delta P_{fl} = \gamma_T H(1-\varepsilon) = \frac{12 G_T}{\pi(D_H^2 + D_H d_0 + d_0^2)}. \quad (2a)$$

From Eq. (2) it follows that for an assigned weight amount of solid phase charged into the equipment (G_T), the drag of the fluidized layer in the conical equipment with the small-section diameter d_0 and the cone aperture α falls off with increase in layer height H, and therefore, with increase in the mass volume flow of the gas. This is accounted for by the fact that in the conical equipment, with increase in porosity, the layer height rises more slowly than its volume, that is, the quantity $(1 - \varepsilon)H$ decreases.

The decrease in ΔP_{fl} with increase in gas mass flow expressed less clearly also occurs in the conico-cylindrical equipment. As an illustration, in Fig. 1 b are presented the curves of pseudo-liquefaction for the conical equipment ($\alpha = 60^\circ$) for a sand heap height of 250 mm of fraction 2 (Fig. 1, 3) and for the conico-

TABLE 1

CHARACTERISTICS OF SAND FRACTIONS

Indicators	Fraction numbers		
	1	2	3
Specific gravity, g/cm^3	2.651	2.657	2.659
Heap weight, g/cm^3	1.639	1.679	1.703
Equivalent diameter of sphere of equal volume, mm	0.163	0.224	0.285
Rate of pseudo-liquefaction, cm/sec:			
in unfilled equipment cross section	2.17	4.60	6.60
in free layer cross section	4.28	8.85	12.73

cylindrical for a heap height of 300 mm of sand in the same fraction (Fig. 1, 4). Also presented for both cases are the curves of the inverse trend (dashed) obtained by gradually reducing the gas mass flow.

In the case of the cylindrical equipment, $\alpha = 0$ and

$$\Delta P_{fl} = \frac{G_T}{\frac{\pi}{4} d_0^2} = \text{const},$$

which corresponds to the familiar principle of the nondependence of fluidized layer drag on gas velocity or mass flow.

For the theoretical calculation of the $\Delta\pi_k$, we assume that the gas flow is distributed uniformly over the layer cross section at any layer height, and that on the pseudo-liquefaction curve there is an acute-angled "pressure peak" (Fig. 1, c). These assumptions naturally entail some deliberate deviation of calculated and experimental values of $\Delta\pi_k$ ($\Delta\pi_{theor}$ and $\Delta\pi_{exp}$).

The pressure drop in the still granular layer with height h_H can be expressed, as we know, by the equation:

$$\Delta P = \zeta \frac{h_H}{d_e} \frac{w^2}{2g} \gamma, \qquad (a)$$

where ζ is the drag coefficient, d_e is the equivalent grain diameter, w is gas velocity, and γ is the specific gravity of the gas.

Since in the granular still and fluidized layers, for sufficiently small particles as usually is the case in fluidized-layer processes, the gas motion regime is laminar: /54

$$\zeta = \frac{C}{\mathrm{Re}} = \frac{C\mu g}{w d_e \gamma},$$

where C = const, μ is gas viscosity, and g is the acceleration due to gravity. Thus,

$$\Delta P = \frac{C\mu}{2d_e^2} w h_{\text{II}} = k w h_{\text{II}}, \qquad \text{(b)}$$

where

$$k = \frac{C\mu}{2d_e^2}.$$

The pressure drop over the elementary path dz (Fig. 2) is: $dP = -kwdz$. If at the heights z and h, where the layer diameters are d and D, the gas velocities are w and w_B, respectively, we have

$$d_0 = d - 2z \operatorname{tg}\frac{\alpha}{2} = D - 2h \operatorname{tg}\frac{\alpha}{2},$$

$$d = D - 2(h - z)\operatorname{tg}\frac{\alpha}{2},$$

$$w = w_B \frac{D^2}{d^2} = w_B \left[\frac{D}{D - 2(h-z)\operatorname{tg}\frac{\alpha}{2}}\right]^2$$

and $$dP = -k w_B D^2 \frac{dz}{\left[D - 2(h-z)\operatorname{tg}\frac{\alpha}{2}\right]^2}.$$

Integrating the last equation in the limits from P_1 to P_2 and from 0 to h_1, and noting that

$$h_{\text{II}} = \frac{D - d_0}{2\operatorname{tg}\frac{\alpha}{2}} = \frac{d_0}{2\operatorname{tg}\frac{\alpha}{2}}\left(\frac{D}{d_0} - 1\right),$$

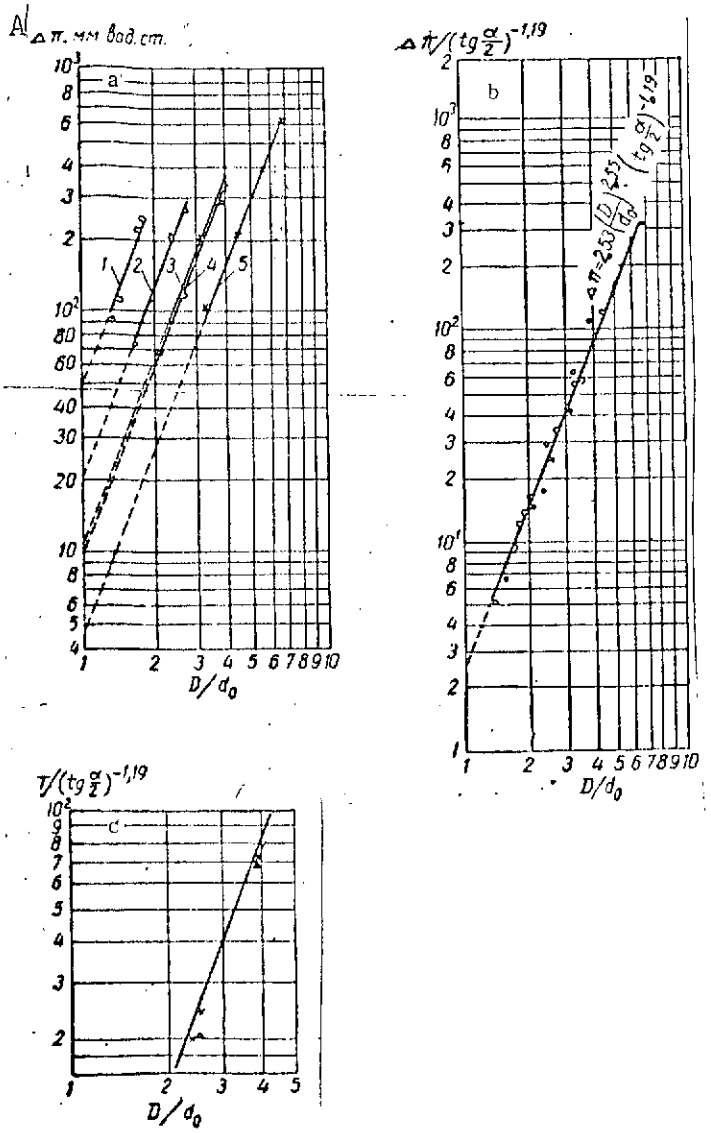

Fig. 3. Experimental functions for "pressure peak"

a. Function $\Delta\pi = f\left(\frac{D}{d_0}\right)$ for different cone apertures

b. Total function $\Delta\pi = f\left(\frac{D}{d_0}, \alpha\right)$

c. Total function $\Delta\pi = f\left(\frac{D}{d_0}, \alpha\right)$ for different sand fractions

Δ is fraction No. 1
V is fraction No. 2
X is fraction No. 3
1. $\alpha = 10^\circ$; 2. $\alpha = 20^\circ$; 3. $\alpha = 30^\circ$;
4. $\alpha = 40^\circ$; 5. $\alpha = 60^\circ$

KEY: A. $\Delta\pi$, mm H_2O

we get: $P_1 - P_2 = \Delta P =$

$$= k w_B \frac{d_0}{2 \operatorname{tg}\frac{\alpha}{2}} \frac{D}{d_0}\left(\frac{D}{d_0} - 1\right). \qquad (3)$$

The maximum pressure drop is observed when the gas velocity in the upper layer cross section corresponds to the beginning of layer expansion ($w_B = w_p$). The "pressure peak" will be expressed as:

$$\Delta\pi_{theor} = \Delta P_{max} - \gamma_H h_H =$$
$$= \frac{d_0}{2 \operatorname{tg}\frac{\alpha}{2}}\left(\frac{D}{d_0} - 1\right) \times$$
$$\times \left(\frac{k w_p D}{d_0} - \gamma_H\right), \qquad (4)$$

where γ_H is the heap specific gravity of the granular material in the still layer. From Eqs. (3) and (4) it follows that

$$\Delta P_{max} = f_1\left(\frac{D}{d_0}, \operatorname{tg}\frac{\alpha}{2}\right);$$
$$\Delta\pi = f_2\left(\frac{D}{d_0}, \operatorname{tg}\frac{\alpha}{2}\right). \qquad (4a)$$

The experimental values of $\Delta\pi$ obtained in the experiments with five different cones

(α = 10, 20, 30, 40, and 60°) for sand chargings up to heights /55
h_H = 100, 150, 200, and 250 mm are shown graphically in Fig. 3 a as a function of D/d_0. The family of straight lines in Fig. 3 a can be expressed by the equation

$$\Delta\pi_{exp} = A_\alpha \left(\frac{D}{d_0}\right)^n, \quad (b)$$

where A_α depends on the cone aperture, decreasing with increase in the cone aperture, and n ≈ 2.5 to 2.6.

Graphical analysis showed that

$$A_\alpha = B\left(\mathrm{tg}\frac{\alpha}{2}\right)^m,$$

where B = const and m ≈ 1.1 to 1.2. Thus,

$$\Delta\pi_{exp} = B\left(\frac{D}{d_0}\right)^n \left(\mathrm{tg}\frac{\alpha}{2}\right)^m. \quad (c)$$

The parameters of Eq. (d) calculated by the least-squares method gives the following values: B = 1.53, n = 2.55, and m = -1.19. Thus, the function (4 a) based on experimental data can be described by the following equation:

$$\Delta\pi = 2{,}53\left(\frac{D}{d_0}\right)^{2{,}55}\left(\mathrm{tg}\frac{\alpha}{2}\right)^{-1{,}19}. \quad (5)$$

Eq. (5), continuous in the range α = 10° to 60° and D/d_0 = 1.30 to 6.77, as we can see from Fig. 3 b, gives a mean deviation from the experimental data within the range of 7.7 percent.

A comparison of the results of calculation based on Eqs. (4) and (5) shows that $\Delta\pi_{theor} < \Delta\pi_{exp}$ in the range $D/d_0 < 2$, but $\Delta\pi_{theor} > \Delta\pi_{exp}$ beyond the limits of this range, where this inequality increases with increase in D/d_0. This situation is due to the fact that in conical and conico-cylindrical equipment

"fluidizing" of the layer occurs not over the entire cross section, but only over the area of the central core, where the latter increases with gas velocity, but remains smaller than the cross-sectional area of the equipment even at high velocities. Therefore, for pseudo-liquefaction /fluidization/ of the layer in the equipment considered, the gas velocity must attain values of w_p only over some portion of the upper cross section of the layer. Here a smaller gas mass flow is required, while the maximum pressure drop is correspondingly less than that calculated based on theoretical formula (4).

From Eq. (b) it follows that the layer drag, including ΔP_{max}, is directly proportional to the velocity of the pseudo-liquefying flow (including also w_p) and is inversely proportional to the square of the diameter of the solid-phase particle d_e^2. Since w_p, like w_k', in turn, is directly proportional to d_e^2, the quantities ΔP_{max} and $\Delta\pi$ must not depend on the dimensions of the particles forming the layer. This principle is confirmed by results of experiments conducted in the conical equipment ($\alpha = 40^\circ$) with the above-indicated three sand fractions. As is clear from Fig. 3 c, the experimental points satisfactorily lie along a straight line described by Eq. (5).

On the other hand, like the pseudo-liquefaction rate, $\Delta\pi$ must increase linearly with increase in the specific gravity of the solid particles in the fluidized layer.

"Fluidizing" of the layer predominantly in the axial core and the ejection of part of the granular material toward the periphery observed in conical and conico-cylindrical equipment is the reason why in this equipment $\Delta P_{fl} < \gamma H$. The point is that the free surface of the layer has an apparently convex shape and the height of the fluidizing core of the layer is less than would be the case for uniform fluidizing of the entire layer, that is, in the absence of a peripheral stagnant zone of nonfluidizing

material. The height of this fluidizing core of the layer (h_d) can be calculated from the measured layer resistance (ΔP_{exp}) and the heap weight of the solid phase (γ_H), that is,

$$h_d = \frac{\Delta P_{exp}}{\gamma_H}.$$

In the case of conicl-cylindrical equipment, the maximum pressure drop must be made up of the drag values of the conical $(\Delta P_{max})_k$ and cylindrical $(\gamma_H h_{cyl})$ layers:

$$\Delta P_{max} = (\Delta P_{max})_k + \gamma_H h_{cyl}; \qquad (d)$$

where $(\Delta P_{max})_k$ is determined by Eq. (5), and h_{cyl} is the height of /56 the heaped (still) sand layer in the cylindrical part of the equipment. For the conico-cylindrical equipment we investigated (Fig. 2), the function expressed by Eq. (d) is represented in Fig. 4 by the section of curve 1 (for the cone) adjoining the inclined line 2 (for the cylinder). Experiments conducted with the three above-indicated sand fractions for charging layer heights h_H = 100 to 450 mm showed that the pressure drop in the cylindrical part of the equipment rises faster than the product $\gamma_H h_{cyl}$ (Fig. 4 1). Here, beginning at some layer height h_0, the increase in ΔP becomes linear, following the product $\gamma_H h_{cyl}$. This effect is accounted for by the fact that the diameter of the fluidizing core in the conical equipment increases with equipment height, but for large values of α it still does not attain the diameter of the large base of the cone. The increase in the diameter of the fluidizing core continues in the cylindrical part of the equipment up to some limiting value, however differing from the diameter of the cylinder by the thickness of the sluggish (or even still) granular material layer observed in equipment with vertical walls. Obviously, until the fluidized diameter core increases, there is

accelerated increase in the actual height of the fluidized layer corresponding to D/d_0 and due to the decrease in the thickness of the peripheral stagnant zone, this causes an accelerated rise in ΔP. Beyond the limits of height h_0 at which the diameter of the fluidizing core is stabilized, the pressure drop rises in proportion to the layer height.

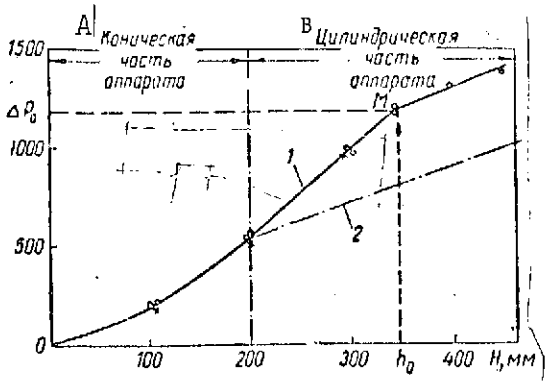

Fig. 4. Dependence of ΔP_{max} on the height of the charged sand layer in conico-cylindrical equipment.
1. Based on experimental data
2. Based on theoretical calculation (for the cylindrical part of the equipment)

KEY: A. Conical part of equipment
B. Cylindrical part of equipment
C. mm

As we can see from Fig. 4, in the conico-cylindrical equipment we investigated, h_0 = 347 mm. In the case when the diameters of the fluidizing core and the cylinder are equal, the layer drag at h_0 = = 347 mm calculated by Eq. (3) would be 1265 mm H_2O. Actually, the pressure drop proved to be 1189 mm H_2O, since the diameter of the fluidizing core is less than the cylinder diameter.

Based on values of ΔP measured in experiments (for w_p = 2.38 cm/sec and k = 0.46), by Eq. (3) we calculated the diameters of the fluidizing core D_0 at different geometrical heights of the equipment investigated, and also the actual heights of the fluidizing layers h_d (Table 2).

Based on the data in Table 2, an outline of the fluidizing core (Fig. 5), which amounts to a body of revolution with a curvilinear contour, was constructed for the conico-cylindrical equipment investigated. We note that the results of experiments figuring in Table 3 and in Fig. 4 confirm the above-mentioned principle that ΔP_{max} does not depend on the size of particles in the fluidizing layer. /57

TABLE 2.

CHARACTERISTIC LAYERS IN CONICO-CYLINDRICAL EQUIPMENT

Height of charged sand layer h_H, mm	P, mm H_2O	h_d, mm	D_0, mm
100	193	68.5	108
197	520	155	129
247	745	194	147
297	962	250	148
347	1189	298	153

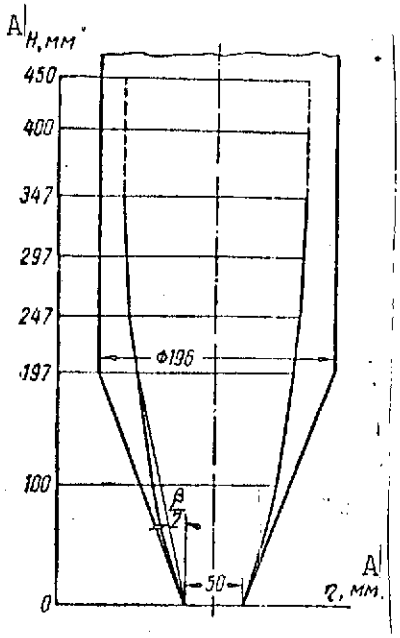

Fig. 5. Profile of fluidizing core in conico-cylindrical equipment
KEY: A. mm

Large "pressure peaks" during /57 pseudo-liquefaction typical of conical and conico-cylindrical equipment (Fig. 1 b) can be avoided by charging the granular material after incorporating the gas flow, that is, in an air jet. This principle was confirmed by experimental data. If we compare the experimental values of the pressure drop in the conical equipment (ΔP_{fl}) with the theoretical pressure drop $\Delta P_{theor} = \gamma h$ and the pressure drops obtained when charging granular material in an air jet (ΔP_c), ΔP_c proved to be the smallest, and ΔP_{theor} proved to be the largest. This is accounted for by the fact that when fed into an air jet the sand is distributed most advantageously from the standpoint of resistance /drag/ to the air flow (effective height of the layer h_d evidently is at a minimum).

We also note that experiments in which sand was charged into a jet were carried out for different air mass flows; no substantial effect of the air mass flow on ΔP_c was observed in this case.